The developmentally regulated ECM glycoprotein ISG plays an essential role in organizing the ECM and orienting the cells of *Volvox*

Armin Hallmann* and David L. Kirk

Department of Biology, Washington University, St Louis, MO 63130, USA
*Author for correspondence at present address: Lehrstuhl für Biochemie I, Universität Regensburg, Universitätsstr. 31, D-93053 Regensburg, Germany
(e-mail: armin.hallmann@vkl.uni-regensburg.de)

SUMMARY

Volvox **is one of the simplest multicellular organisms with only two cell types, yet it has a surprisingly complex extracellular matrix (ECM) containing many region-specific morphological components, making** *Volvox* **suitable as a model system for ECM investigations. ECM deposition begins shortly after inversion, which is the process by which the embryo turns itself right-side-out at the end of embryogenesis. It was previously shown that the gene encoding an ECM glycoprotein called ISG is transcribed very transiently during inversion. Here we show that the developmentally controlled ISG accumulates at the bases of the flagella right after inversion, before any morphologically recognizable ECM structures have yet developed. Later, ISG is abundant in the 'flagellar hillocks' that encircle the basal ends of all flagella, and in the adjacent 'boundary zone' that delimits the spheroid. Transgenic** *Volvox* **were generated which express a truncated form of ISG. These transgenics exhibit a severely disorganized ECM within which the cells are embedded in a highly chaotic manner that precludes motility. A synthetic version of the C-terminal decapeptide of ISG has a similar disorganizing effect, but only when it is applied during or shortly after inversion. We postulate that ISG plays a critical role in morphogenesis and acts as a key organizer of ECM architecture; at the very beginning of ECM formation ISG establishes an essential initial framework that both holds the somatic cells in an adaptive orientation and acts as the scaffold upon which the rest of the ECM can be properly assembled, assuring that somatic cells of post-inversion spheroids are held in orientations and locations that makes adaptive swimming behavior possible.**

Key words: EM-immunolocalization, Embryogenesis, Extracellular matrix, Green alga, Green flagellate

INTRODUCTION

The extracellular matrix (ECM) frequently does much more than hold the cells of a multicellular organism in place; often it serves as a conduit for signals passing between cells of different types, thereby mediating a variety of developmental and physiological responses, regulating cellular growth, differentiation, and proliferation, initiating wound repair and pathogen defenses, and so on. The spherical green flagellate *Volvox carteri* has many features that recommend it as a model system for studying these and other aspects of ECM biology.

In terms of cellular composition, *V. carteri* is about as simple as a multicellular organism can be. It has only two cell types: 2,000-4,000 small, terminally differentiated, biflagellate somatic cells near the surface of the spheroid, and ~16 large, potentially immortal asexual reproductive cells (called 'gonidia') just internal to the somatic cell layer. But >99% of a mature *Volvox* spheroid is ECM, and for an organism that is otherwise so simple, its ECM is surprisingly complex. It is composed principally of an assortment of hydroxyproline-rich glycoproteins (HRGPs) many of which are extensively sulfated (reviewed by Sumper and Hallmann, 1998). These HRGPs are organized into a set of highly regular fibrous layers that coat the spheroid, form a honeycomb-like array of cellular compartments that house the somatic cells, enclose each gonidium, and surround a voluminous central region that (like each of the cellular compartments) is filled with a loose feltwork of HRGP fibers and filaments (Kirk et al., 1986).

The ECM has at least two identifiable roles in regulating *V. carteri* development: (i) It promotes gonidial growth and maturation, presumably by acting as a storage site for nutrients; gonidia grow twice as fast when surrounded by an intact ECM as they do when the ECM has been ruptured mechanically (Koufopanou and Bell, 1993). (ii) It plays some kind of critical (but as yet poorly understood) role in the pheromone-dependent process by which the organism is switched from asexual to sexual reproduction (reviewed by Hallmann et al., 1998); it takes 100× as much pheromone to trigger sexuality in isolated gonidia as in gonidia that remain in an intact spheroid (Wenzl and Sumper, 1987).

The *Volvox* ECM is particularly interesting from a phylogenetic point of view. Numerous lines of evidence indicate that *Volvox* has evolved from a unicellular ancestor similar to *Chlamydomonas reinhardtii* during the past ~50 million years (Rausch et al., 1989), and that during this period the *Volvox* ECM has evolved by modification and elaboration of the simple cell wall of its chlamydomonad ancestor (reviewed by Kirk, 1998; Kirk, 1999). Indeed, the HRGPs of

the outermost ('crystalline') layers of the *C. reinhardtii* cell wall and the *V. carteri* ECM remain so similar in structure and assembly properties that they are capable of substituting for one another in an in vitro reassembly system (Adair et al., 1987). Other HRGPs of the two organisms exhibit sequence similarities that suggest that the family has evolved by extensive exon shuffling (Sumper and Hallmann, 1998; Woessner et al., 1994). These observations indicate that *Chlamydomonas* and *Volvox*, together with their relatives of intermediate complexity in the family Volvocaceae (Starr, 1980), offer an unrivalled opportunity to explore the way in which a complex ECM has evolved from a simple cell wall.

However, the *Volvox* ECM is at least as interesting and accessible as a developmental model system as it is as an evolutionary model system: in each asexual life cycle, *V. carteri* gonidia act like stem cells, dividing to produce juvenile spheroids containing a new cohort of gonidia and somatic cells embedded in a new ECM (Starr, 1969). Because construction of this new ECM begins at a well-defined point in the life cycle – immediately after the end of embryogenesis – and because the life cycle can be synchronized with a light-dark cycle, *V. carteri* provides a unique opportunity to study ECM synthesis and assembly in a synchronous system.

In outline form, the *V. carteri* asexual life cycle is as follows (Starr, 1969; Starr, 1970): each mature gonidium initiates a series of 11-12 rapid cleavage divisions, a subset of which are visibly asymmetric and set apart large gonidial initials from small somatic initials. By the end of cleavage, therefore, all of the cells of both types that will be present in an adult of the next generation have been produced, but at this stage they constitute a syncytium in which all of the cells are joined by numerous cytoplasmic bridges that were produced as a result of incomplete cytokinesis. At this stage the embryo is also inside out with respect to the adult configuration: the gonidia are on the outside, and the flagellar ends of the somatic cells all point inward. This condition is quickly corrected, however, as the embryo turns right-side-out in a gastrulation-like morphogenetic process called inversion, which takes ~40 minutes, and in which the cytoplasmic bridges play a crucial role (Viamontes et al., 1979). The embryonic cells are completely devoid of ECM during cleavage and inversion, but initial deposition of ECM can be detected microscopically shortly after inversion. It is critical that construction of a coherent ECM proceed quickly at this stage, because soon the cytoplasmic bridges will break down, and in the absence of an ECM capable of holding the cells in place, the juvenile will fall apart. It is also important that the ECM form in such a way that all somatic cells are held in a similar orientation with respect to the anterior-posterior axis of the spheroid (just as they are initially in the embryo), because it has been shown that if this is not the case, the spheroid is incapable of swimming (Huskey, 1979), which would be lethal in the natural environment. Once initiated, ECM deposition continues for several days, causing the spheroid to expand (in the absence of any further cell division) and the somatic cells to move apart like points on an expanding balloon. Part way through their expansion process, the progeny spheroids digest their way out of the parental ECM and become free-swimming adults in which the gonidia will soon initiate a new round of embryonic development. By the time its progeny swim away, the parental spheroid will have undergone a prodigious ~50,000-fold increase in volume, but within just a few more hours its somatic cells will be dead, and they and the ECM surrounding them will both undergo complete dissolution.

In-vivo-pulse-labeling studies revealed that ECM biosynthesis begins during inversion with the synthesis of a single glycoprotein that is called 'inversion-specific glycoprotein,' or ISG, and that has some remarkable properties (Schlipfenbacher et al., 1986; Wenzl and Sumper, 1982). ISG is a sulfated glycoprotein containing an N-terminal globular domain of unnoteworthy amino acid composition, plus a C-terminal hydroxyproline-rich domain containing numerous Ser-$(Hyp)_{4-6}$ repeats (Ertl et al., 1992). Because most of the hydroxyamino acids in the C-terminal domain are glycosylated (with the dominant sugars being arabinose and galactose), this domain assumes the form of a rigid 57 nm rod. Purified ISG oligomerizes to form star-like particles with a central knob and a variable number of 57 nm arms, indicating that ISG molecules have a propensity to associate via their globular N-terminal domains. A sequence-homology search turns up only one putative homologue of ISG: a *C. reinhardtii* cell wall glycoprotein called VSP-3 (Woessner et al., 1994). Remarkably, although the N-terminal globular domains of ISG and VSP-3 are highly similar, the rod-shaped domain of ISG with its Ser-$(Hyp)_{4-6}$ repeats is replaced in VSP-3 by a totally different rod-shaped domain containing numerous $(Ser-Hyp)_n$ repeats.

The most impressive feature of ISG is that the gene encoding it is under extremely tight developmental control: it is transcribed for only a 10 minute period during inversion (Ertl et al., 1992)! But although ISG mRNA is synthesized only transiently, ISG accumulates in the ECM for some period of time, and is stable for at least 24 hours (Wenzl and Sumper, 1982). Indirect immunofluorescence microscopy revealed that ISG is located in the ECM near the surface of the somatic cell layer (Ertl et al., 1992), but in that study a more precise localization was not possible.

In this paper we use fine-structure immunocytochemistry to study the initial stages of ISG deposition, to localize the protein more precisely within the ECM of young adult spheroids, and to study the developmental effects of expressing a transgene encoding a truncated ISG that lacks the N-terminal globular domain. The phenotype of this transgenic *Volvox* is then compared to the phenotype generated in the presence of a synthetic version of the C-terminal decapeptide of ISG (CTD), which was previously shown to interfere with spheroid morphogenesis (Ertl et al., 1992). The results indicate clearly that ISG plays an essential role during initial stages of ECM deposition in establishing the normal architecture of the ECM, and assuring that the somatic cells remain oriented in an adaptive manner within the developing ECM.

MATERIALS AND METHODS

Volvox strains and culture conditions

The female *Volvox carteri* f. *nagariensis* strains 'Eve' (wild-type) and '153-48' (*nit*A⁻) were grown synchronously in *Volvox* medium (Provasoli and Pintner, 1959) at either 28°C or 32°C on an 8 hours dark/16 hours light (10,000 lux) cycle (Starr and Jaenicke, 1974). Strain 153-48 was grown in medium containing 1 mM NH_4Cl.

Isolation of *Volvox* embryos and juveniles

Volvox spheroids were harvested at the stage of embryogenesis by filtration on a 90-μm mesh nylon screen, broken in a Dounce homogenizer with a loose-fitting pestle, and filtered on a 90-μm mesh nylon screen, which allows the free embryos, plus small fragments of the somatic-cell layer to pass. The embryos were then separated from residual somatic cells and ECM fragments by successively washing on a 30-μm mesh nylon screen, centrifuging for 2 minutes at 500 *g* in 70 μl/ml Percoll (Pharmacia, Uppsala, Sweden), decanting, and then washing 3× with *Volvox* medium at unit gravity. In most cases when prehatching juvenile spheroids were to be studied, embryos were isolated as above and then incubated until they had reached the stage of interest.

Peptide synthesis

The peptide KKKATGRRLL (the C-terminal decapeptide of ISG; CTD) was synthesized by using 9-fluorenylmethyloxycarbonyl amino acid derivatives. The peptide was purified on a reversed phase C_{18} HPLC-column (Nucleosil 100-7, 7 μm; Macherey-Nagel, Düren, Germany). The sequence of the peptide was confirmed by Edman degradation using an automated gas phase peptide sequencer (Applied Biosystems, Foster City, CA).

Preparation of anti-ISG antibodies

Three peptides were used as immunogens to produce polyclonal antibodies in rabbits. Two were fragments representing residues 5-172 at the amino end, and residues 402-464 at the carboxy end of the mature ISG molecule; these were produced by expressing the appropriate regions of the ISG cDNA in *E. coli* (Ertl et al., 1992). The third was CTD, the KKKATGRRLL peptide described above, attached via its C terminus to bovine serum albumin as a carrier. IgG fractions from the resulting sera were purified by Protein A-Sepharose column chromatography (Pharmacia, Uppsala, Sweden), and tested for specificity by western blot analysis.

Construction of a truncated ISG gene

A truncated ISG gene lacking the N-terminal domain was generated by a recombinant PCR technique (Horton et al., 1989), in which the PCRs were performed as previously described (Hallmann and Sumper, 1994). The first PCR was performed on the genomic ISG sequence with an 18-mer 5′-sense primer (5′-TAAGTAGTAACACG-TACG) and a 43-mer 3′-antisense primer (5′-<u>GTTGTCTGTACGAC-GACCGC</u>*GATGTTGTTGTAGACGCTTACAG*) in which one half (italicized) is complementary to the beginning of exon 2, and the other half (underlined) is complementary to the beginning of exon 3. The second PCR was performed on the same template with a 43-mer 5′-sense primer that is the complementary to the 43-mer primer used in the first PCR (5′-*CTGTAAGCGTCTACAACAACATC*<u>GCGGTCGTC-GTACAGACAAC</u>), plus a 19-mer 3′-antisense primer (5′-GAGGAG-AGGAAACTGGCTG). The third PCR was carried out with the first two PCR products and the flanking primers; it resulted in a 723-bp fragment. Two unique restriction sites within this fragment, *Hin*dIII and *Mlu*I, were used for connection to the flanking sequences, just as they were with the wild-type ISG gene, and the final construction was performed by standard techniques (Sambrook et al., 1989). All products were verified by sequencing.

Stable transformation of *Volvox*

Co-transformation of *Volvox* was performed as described (Schiedlmeier et al., 1994), except that a Biolistic PDS-1000/He-particle gun (Bio-Rad) (Hallmann et al., 1997) was used to bombard strain 153-48 (*nitA⁻*) with 1 μm gold beads (Bio-Rad) that had been coated with DNA encoding the selectable marker (*nitA*) plus the unselected marker (the truncated ISG gene).

Genomic PCR and reverse-transcription PCR

Genomic PCR was used to test Nit[+] transformants for the presence of the unselected marker. Fifty spheroids were selected under a stereomicroscope and transferred into 10 μl of sterile lysis buffer (0.1 M NaOH, 2.0 M NaCl, 0.5% SDS). After 5 minutes at 95°C, 200 μl of 50 mM Tris-HCl, pH 7.5, were added, and 2 μl of the resulting lysate was used for PCR in a total volume of 100 μl. Reverse-transcription (RT-) PCR was used to test for the presence of recombinant mRNA in transformants, as previously described (Hallmann and Sumper, 1994). Products of PCR amplification were cloned into the *Sma*I site of pUC18 or pBluescript II SK and sequenced.

## Preparation of *Volvox* specimens for fine-structure immunocytology

Exept where stated otherwise, immunocytological studies were performed with the wild-type female strain, Eve. Because there had been no previous reports of successful immunocytological studies of *Volvox* at the EM level, we tested a series of alternative procedures at every step of specimen preparation. For example, ~50 different protocols for counterstaining the ECM with Ruthenium red, and/or 3,3′-diaminobenzidine, and/or various heavy-metal salts – all at a range of concentrations, with a range of staining times, and in different sequences – were tested, using grids that had already been well stained with primary and secondary antibodies. All such variants were evaluated in the EM with respect to their effects on the signal-to-noise ratio obtained with the immunogold staining, and their effects on preservation and visualization of ECM architecture. Shortly we will describe in detail the protocol that we found gave the best overall results. But because this is the first EM-immunolocalization study to be reported for *Volvox*, we believe it may be useful to first comment briefly on the relative merits of some of the most significant variables that we tested.

Of the fixatives tested, a mixture of 4% paraformaldehyde and 0.25% glutaraldehyde turned out to provide the best compromise between well-preserved fine structure and well-preserved immunoreactivity. Unicryl (BBInternational, Cardiff, UK) gave much better results as an embedding resin than either Lowicryl K4M or Spurr's low viscosity resin. This is probably because polymerized Unicryl, being relatively hydrophilic, leaves the biological components in thin sections more accessible to aqueous staining and incubating solutions, particularly the antibodies.

Following antibody staining, specimens were counterstained sequentially with ruthenium red, osmium tetroxide, uranyl acetate and lead citrate, since this combination and sequence of heavy metal stains provided the clearest images of ECM fine structures. In the course of these studies we discovered, however, that not all of the morphological features of the ECM that were previously observed in mature *V. carteri* spheroids (Kirk et al., 1986) are present in the younger specimens studied here. Nor are all of the ECM details that are revealed at any given stage of development using conventional EM-preparative methods equally well revealed when specimens have been prepared using methods designed to preserve immunoreactivity. Nevertheless, when specimens of the same stage were prepared by the methods outlined below and by the methods previously reported (Kirk et al., 1986), a satisfactory correspondence in ECM details was obtained (data not shown).

The methods used to prepare specimens for EM-immunolocalization of ISG were as follows: (Where not otherwise specified, all treatments took place at a temperature of 22°C.) Specimens (whole spheroids or isolated embryos or juveniles) were fixed in 4% paraformaldehyde and 0.25% glutaraldehyde in 0.1 M cacodylate buffer (pH 7.3) for 90 minutes. After three 30-minute washes in 0.1 M cacodylate buffer, the spheroids were dehydrated by passage (10 minutes each) through 50% EtOH, 70% EtOH, 90% EtOH, and 100% EtOH 3×. Specimens were infiltrated in Unicryl (BBInternational, Cardiff, UK): EtOH (1:2) for 30 minutes, in Unicryl: EtOH (2:1) for 30 minutes, and in pure Unicryl for 1 hour, followed by six changes of Unicryl of ~12 hours each. Specimens in

Fig. 1. Diagrammatic representation of the relationships among
several relevant portions of the ECM in the vicinity of the
somatic cells (SC) of an adult spheroid of *Volvox carteri*. Four
main zones of the *Volvox* ECM are recognized (Kirk et al.,
1986): the flagellar zone, the boundary zone, the cellular zone,
and the deep zone. The flagellar zone (FZ), includes all ECM
specializations seen on or in the immediate neighborhood of
the flagellum. The only FZ subzone that is seen clearly in the
present study is the 'flagellar hillock,' FZ3a. The boundary
zone (BZ) includes all components of the ECM that, except in
the periflagellar regions, appear to be continuous over the
surface of the organism, but are not structurally continuous
with deeper layers. The only subzone of BZ that is seen clearly
in the present study is its innermost layer, BZ3; it abuts FZ3a.
The CZ includes all ECM components that are internal to the
boundary zone and that exhibit specializations around the
individual cells. Its subzones are CZ1: the coherent meshwork
of ECM filaments attached to the plasmalemma of each cell body, CZ3: the distinct fibrous material that creates a compartment surrounding
each of the individual cells, and CZ2: the relatively amorphous components filling the space between CZ1 and CZ3. The deep zone (DZ)
contains all ECM components internal to the CZ; although it is the largest region of the *V. carteri* ECM, it was not found to be relevant to the
present report, and hence is not shown.
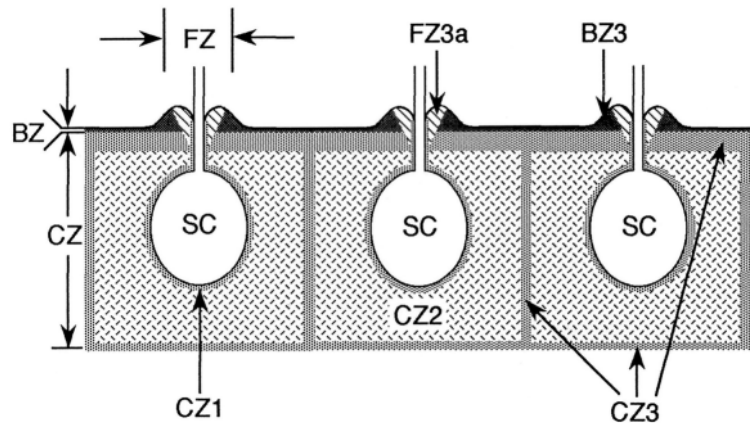
resin were transferred to BEEM-capsules (Electron Microscopy
Sciences, Fort Washington, PA) and the resin was then polymerized
by exposure to 360 nm light on dry ice for 72 hours, followed by a
12-hour exposure at room temperature after removal of the
polymerized blocks from the BEEM-capsules.

Ultrathin sections (~80 nm) of the Unicryl-embedded specimens
were cut using a MT-2 Porter-Blum ultramicrotome (Sorvall,
Norwalk, CT) and diamond knife (du Pont de Nemours, Wilmington,
DE). Sections were transferred to Formvar-coated nickel grids (200
mesh), stabilized with evaporated carbon film (Electron Microscopy
Sciences, Fort Washington, PA), floated section-side down first on
drops of 20 mM Tris-HCl, pH 7.4, 225 mM NaCl (TBS) containing
0.1 M glycine for 10 minutes, and then on TBS with 5% Tween-20
and 1% fish gelatin (blocking solution 1) for 30 minutes. Grids were
labeled by exposure for 20 hours to purified primary antibodies at 30
μg/ml in blocking solution 1, and then washed 5× 3 minutes in TBS
with 0.5% Tween. They were then reblocked for 10 minutes with TBS
at pH 8.2 with 0.05% Tween-20, 1% fish gelatin (blocking solution
2) before being incubated 4 hours with gold-labeled secondary
antibody (goat anti-rabbit IgG on 10 nm colloidal gold particles; Ted
Pella, Redding, CA) 1:20 in blocking solution 2 that also contained 1
mg/ml goat IgG (Sigma, St Louis, MO). Grids were next washed 5×
3 minutes in 20 mM Tris-HCl, pH 8.2, 2.25 M NaCl, and then 5× 3
minutes in distilled water (DW). The antibodies were fixed to the
sections in 1% aqueous glutaraldehyde for 10 minutes. Grids were
then washed again 5× 3 minutes in DW and then counterstained with
filtered 0.5% ruthenium red (Luft, 1964) in 20 mM Tris-HCl, pH 7.4,
for 90 minutes at 55°C, washed 5× 3 minutes in DW, incubated in 2%
OsO$_4$ for 1 hour, rinsed quickly 3× in DW and washed again 5× 3
minutes in DW, stained with filtered 2.5% uranyl acetate for 10
minutes in the dark and washed again in DW. Final staining was in
filtered 4 mg/ml lead citrate in carbonate-free DW (Venable and
Coggeshall, 1965). Finally, grids were washed in DW, dried, and
examined in a H-600 transmission electron microscope (Hitachi,
Tokyo, Japan) at 75 kV.

RESULTS

Structure and nomenclature of the *V. carteri* ECM

A comparative EM study of adult spheroids representing four
recognized divisions of the genus *Volvox* was used to devise
the system of nomenclature that is presently used to identify
four main zones and several anatomically distinct subzones of

the *Volvox* ECM (Kirk et al., 1986). The zones and subzones
that will be referred to in the present report are illustrated in
Fig. 1, and defined in the caption to that figure.

The earliest stage in ECM assembly: deposition of ISG at the flagellar bases

As noted in the introduction, the first indication of
imminent ECM deposition occurs when ISG mRNA is
briefly transcribed during embryo inversion. We therefore
wished to determine how soon after inversion – and where –
ISG begins to accumulate in the extracellular space. To this
end, embryos were isolated during early cleavage, monitored
microscopically during the rest of embryogenesis and samples
were fixed for immunocytological examination immediately
after inversion, and then 60 and 180 minutes later. Although
inversion normally occurs in the dark under the light-dark cycle
that is used to synchronize development, for this experiment
inverting and postinversion embryos were incubated in the
light, because it is known that protein synthesis in *V. carteri* is
strongly light dependent (Kirk and Kirk, 1983; Kirk and Kirk,
1985).

Antibodies elicited by all three of the immunogens described
in the Materials and Methods section were tested for specificity
with western blots and shown to be ISG-specific. The result
with two of these antibodies is presented in Fig. 2. Neither
antibody detects any band in samples taken 2 hours before
inversion, but they both detect a single band corresponding to
ISG in samples taken 2 hours after inversion (apparent
molecular mass of ISG: ~200 kDa).

When used for fine structure immunocytochemistry with
Volvox embryos before inversion all ISG antibodies did not
give any significant immunostaining. When *Volvox* embryos
after inversion were used all ISG antibodies gave essentially
the same staining pattern, but both of the antibodies elicited
with C-terminal immunogens gave stronger signals than the
one elicited with the N-terminal immunogen. The antibody
preparation elicited with CTD (the C-terminal decapeptide of
ISG) was used in the study about to be reported, and all other
immunolocalization studies reported further below.
Background immunogold staining was assessed in specimens
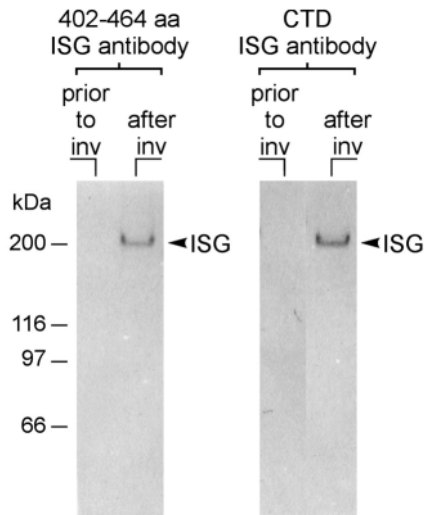in which the primary antibody was replaced by buffer and was

Fig. 2 is at the top-left of the page:

**402-464 aa
ISG antibody**

prior
to   after
inv   inv

**CTD
ISG antibody**

prior
to   after
inv   inv

kDa

200 — ◄ISG   ◄ISG

116 —

97 —

66 —

Fig. 2. Specificity of ISG antibodies. Western blot analysis of wild-type *Volvox* embryos 2 hours prior to inversion and 2 hours after inversion. Total SDS-soluble protein was fractionated on an 8% SDS-polyacrylamide gel, electroblotted and probed using the antibody against amino acids 402-464 of ISG (402-464 aa ISG antibody) or the antibody against CTD (CTD ISG antibody), the KKKATGRRLL peptide of ISG. The antigen-antibody complex was detected using alkaline-phosphatase-conjugated secondary antibodies. The apparent molecular mass of ISG is know to be ~200 kDa on an 8% SDS-polyacrylamide gel (Schlipfenbacher et al., 1986). ISG was only detectable after inversion.

found to be extremely low. Negative controls included replacement of the ISG-specific IgG with IgGs derived from the preimmune serum, an antiserum to a human protein, and three antisera raised against three different *Volvox* cellular antigens. The first two of these controls produced no immune staining, and the last three produced no staining within the ECM.

Fine structure immunocytology with embryos fixed immediately after inversion revealed the presence of ISG on the surface of the somatic cells at the bases of the flagella (approximately where the flagellar hillock, flagellar zone (FZ) 3a, is located in the mature spheroid) before any other structural elements of the ECM could be discerned (Fig. 3A). By one hour postinversion, ECM components belonging to the developing boundary zone (BZ) and cellular zone (CZ) are becoming visible (albeit without recognizable substructure), but the most electron-dense region of the ECM continues to be the flagellar hillock region, where immunogold staining is also most intense (Fig. 3B). Three hours after inversion various components of the ECM have developed somewhat further, and ISG has become detectable in two regions of the boundary zone: next to the flagellar hillock and at the point where two somatic-cell compartments meet (Fig. 3C,D). At these early stages of ECM formation, ISG deposition and flagellar hillock formation never appeared to occur symmetrically around the flagellar bases; rather, both seemed to occur initially on just one side of the flagellum (see Fig. 3C, for example). So far, however, we have been unable to determine whether ISG deposition regularly begins on one particular side of the flagellum, and if so which side this is. Our guess is that ISG deposition probably begins on the side distal to the adjacent

flagellum, but serial sectioning may be required to determine unambiguously whether this is the case.

In older spheroids ISG is abundant in the boundary zone as well as in the flagellar hillock

In 18-hours-postinversion spheroids, ISG (as revealed by immunogold labeling) continues to be abundant in the flagellar hillocks. This is obvious both in sections that are cut perpendicular to the surface of a spheroid (Fig. 4), and in sections cut tangential to the surface, within which each hillock appears as a ring-like structure encircling a flagellum (Fig. 5). By this stage, however, there is also substantial immunogold labeling of the inner surface of the BZ (Figs 4A, 6). Although the subzones of the fully mature BZ that were previously described (Kirk et al., 1986) cannot be visualized at this stage of development using the preparative methods developed here for immunolocalization purposes, the immunogold labeling seen in Fig. 6 clearly is restricted to the very inner surface of the BZ, which is how BZ3 was defined. As with the very young postinversion juveniles, in these 18-hours-postinversion embryos no immunogold staining above background levels was observed in the vicinity of the gonidia, within the deep zone, or anywhere else in the ECM (data not shown). Thus, we conclude that ISG appears to be localized exclusively in the flagellar hillocks (FZ3a) and the inner layer of the boundary zone (BZ3).

Expression of a truncated ISG leads to a disorganized ECM architecture

To learn more about the function of ISG, transgenic *Volvox* were generated that express a truncated ISG. Since purified ISG molecules associate via their N-terminal globular domains to form star-like oligomeric particles, we chose to delete the N-terminal domain. The genomic clone of ISG derived from wild-type *V. carteri* (Ertl et al., 1992), was used for this purpose. In the final construct nearly the entire N-terminal domain (as well as the second intron) was deleted (for details see Materials and Methods and Fig. 7A). The resulting construct begins ~1.1 kb upstream of the ATG initiation codon and ends ~1.4 kb downstream of the stop codon. Thus the truncated gene remains associated with the native ISG promoter, which should cause it to be transcribed like the wild-type ISG gene: for only ~10 minutes during inversion (Ertl et al., 1992; Schlipfenbacher et al., 1986).

A morphologically wild-type, *nitA⁻* mutant of *V. carteri* (strain 153-48) was co-bombarded with the construct carrying the truncated ISG gene and a *nitA* plasmid, to achieve co-transformation as previously reported (Hallmann and Sumper, 1994; Schiedlmeier et al., 1994). Normally, integration of plasmid DNA into the *Volvox* genome occurs by non-homologous recombination at sites other than the corresponding wild-type gene (Hallmann et al., 1997), therefore transformants should express the truncated plus the wild-type ISG gene, but might synthesize more truncated ISG than wild-type ISG, since integration of plasmid DNA often occurs in multiple copies (Schiedlmeier et al., 1994).

PCR with genomic DNA from *nitA⁺* transformants was used to test for the presence of the truncated ISG gene. Nine out of 18 independent *nitA⁺* transformants that were tested contained the truncated ISG gene (data not shown). The RT-PCR technique was then used to test for the presence of the expected

Fig. 3. Immunolocalization of ISG in embryos fixed immediately after inversion (A), 60 minutes postinversion (B) or 180 minutes postinversion (C,D). (A,B and C,D) Representative results of three independent experiments. In all four cases the plane of section is perpendicular to the surface of the embryo; in three cases it passes longitudinally through a flagellum of a somatic cell (A,B,C), and in the fourth it passes through the junction between two somatic cell compartments (D). The gold particles attached to the secondary antibody are 10 nm in diameter. (A-C) Numerous gold particles reveal the presence of ISG within the developing flagellar hillocks (FZ3a), but at these early stages ISG deposition and hillock formation appear to occur preferentially on only one side of each flagellum (C). By 3 hours postinversion, ISG accumulation is also observed within the boundary zone in two regions: next to FZ3a (C) and at the junction between two somatic cell compartments (D). In these early stages of ECM formation, clear distinctions cannot yet be made between the inner edge of BZ and the outer edge of CZ, or between CZ1, CZ2 and CZ3. Nevertheless, it appears certain that the CZ region marked with a pair of arrowheads in D is destined to become the portion of CZ3 that will form the fused walls of two adjacent somatic cell compartments. F, flagellum; BB; basal body; TZ, transition zone between BB and the axoneme of the flagellum; other labels as in Fig. 1. Bars, 100 nm.
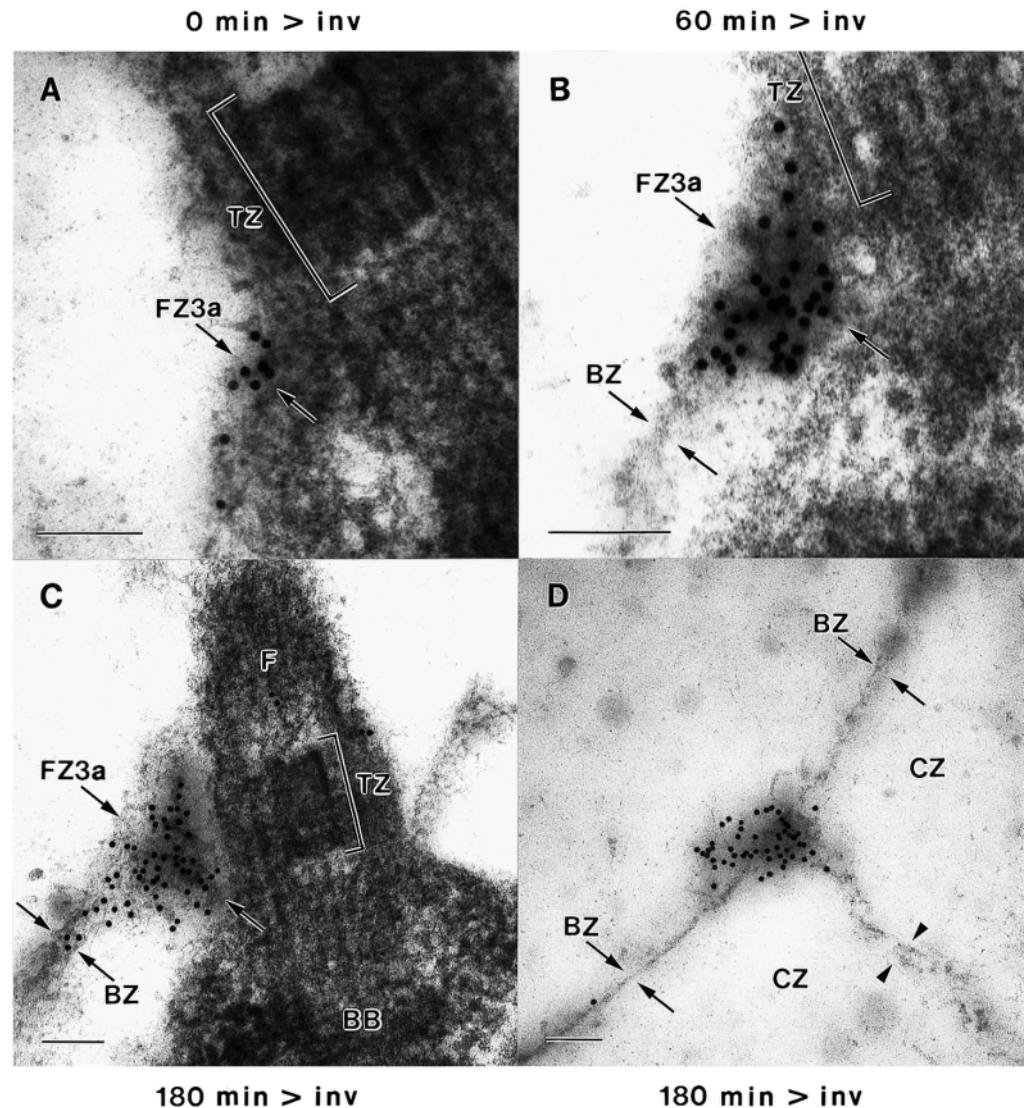
truncated ISG mRNA, at the expected stage of development in the transgenic strains. To that end, RNA extracted from inverting embryos of all nine cotransformant lines was subjected to RT followed by PCR, using primers that should amplify the portion of the ISG mRNA containing both the putative deletion and the region where intron 1 is still present in the construct. It was predicted that transformants that transcribed the truncated ISG gene and processed the resulting transcript properly (to remove intron 1 cleanly) should yield a 224 bp RT-PCR product. An RT-PCR product of this size was recovered from four of the nine transformants. The result with one of the four RT-PCR-positive transformants is shown in Fig. 7B. Moreover, RNA samples isolated from the same four strains, but at developmental stages other than during inversion, failed to yield a 224-bp-RT-PCR fragment, indicating that the truncated transgene was subject to the same sort of developmental regulation as the wild-type allele. In addition, the truncated version of the ISG transcript cannot be detected in the parental strain from which the transformants were derived (Fig. 7B). When the RT-PCR products of the four

positive transformants were cloned into pBluescript II and sequenced, they all turned out to have exactly the predicted sequence for RT-PCR products derived from a properly transcribed and processed truncated-ISG mRNA (Fig. 7C).

The five co-transformant strains that contained an integrated copy of the truncated ISG gene, but failed (for some unknown reason) to express it in a way that resulted in recovery of the predicted RT-PCR product, were all morphologically similar to the parental strain (153-48). In marked contrast, all four of the transformants that expressed the truncated ISG gene in the predicted manner exhibited a similar bizarre phenotype as adults (Fig. 8), revealing a one-to-one correspondence between expression of a truncated gene and a seriously perturbed morphology. These four transgenic strains are all incapable of swimming, and even when they are viewed at low power it is obvious that their spheroids are highly disorganized (Fig. 8B).

At higher power it becomes obvious that the transgenic somatic cells are oriented and positioned randomly, and that far from being positioned at the outer edge of the ECM they are buried deeply within it (Fig. 8D,F). Buried so far from the
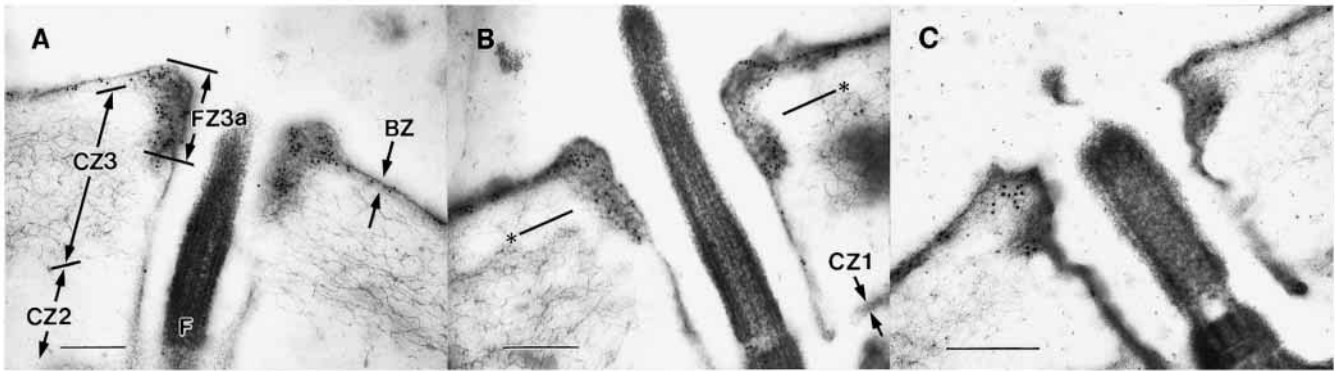
Fig. 4. Immunolocalization of ISG in the ECM adjacent to somatic cells of 18-hours-postinversion spheroids in three independent experiments. All three sections were cut perpendicular to the spheroid surface and pass longitudinally through a flagellum. In each micrograph numerous gold particles reveal the presence of abundant ISG within the flagellar hillocks (FZ3a) and the boundary zone (BZ). Labels as in Figs 1, 3. The two asterisks in B indicate the approximate plane of section for the specimens shown in Fig. 5. Bars, 300 nm.

surface, and in such randomized orientations, it is little wonder that these flagella are incapable of moving the spheroid, no matter how hard they beat.

Examination of embryos before and after inversion provides significant insight into the developmental origin of the phenotypic abnormality of the transgenic adults. Prior to inversion, (while the embryonic cells are all held in fixed relationships by the cytoplasmic bridges that link them), the transgenic embryos are indistinguishable from wild-type embryos (Fig. 8D). But a few hours after inversion (which is when cytoplasmic bridges break down and the task of holding the cells in fixed relationships is normally taken over by the ECM), all regularity of cellular orientations is suddenly lost (Fig. 8F). This observation led to the working hypothesis that when a truncated version of ISG lacking the N-terminal domain is present, it acts as a 'dominant-negative' molecule that interferes with a critical role that the wild-type ISG molecules normally play in organizing the ECM at very early stages of its assembly.

EM-level ISG-immunolocalization studies of transgenic spheroids yielded results consistent with the preceding hypothesis (because only the N-terminal domain is missing from the transgene product, and the antibody used in all immunolocalization studies reported here is directed toward the C-terminal decapeptide of ISG, it was anticipated that it would recognize the transgene product about as well as the wild-type ISG). The ECM of transformants is grossly perturbed (Fig. 9). The flagellar hillocks, which normally are the sites where ISG is first detected, and where it ultimately becomes most abundant, are not seen in these transformants. While there are structures that resemble boundary zone fragments present near the somatic cells of the transgenic spheroids, and although these structures are labeled with immunogold as the wild-type BZ is, such material is by no means restricted to the region where the BZ is normally located. Rather, it extends outward in loose, ill-defined swirls, well beyond what is normally the outer limit of the ECM (arrowheads in Fig. 9A-C). In short, it appears that in the presence of a truncated form of ISG *V. carteri* is no longer able to generate a coherent BZ that holds the somatic cells in place and acts as a true boundary zone that delimits the ECM.

The C-terminal decapeptide of ISG perturbs the initial steps of ECM construction

In the preceding study it was not possible to control when, or at what concentration, the truncated form of ISG was present.
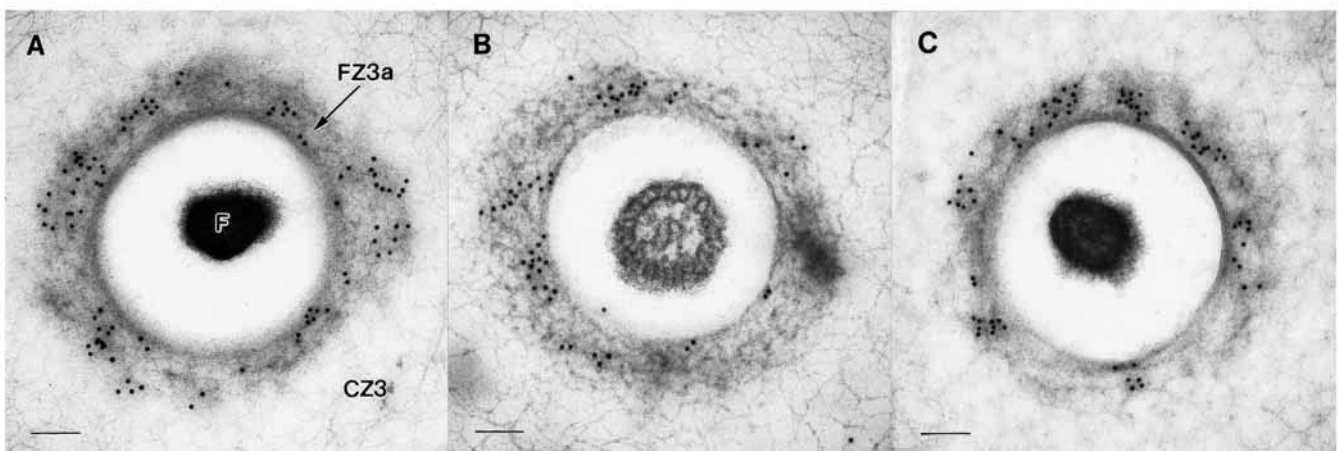

Fig. 5. Immunolocalization, in three independent experiments, of ISG in tangential sections of 18-hour-old spheroids. All sections pass through a flagellum and a flagellar hillock (FZ3a) at approximately the level indicated in Fig. 4B. Numerous gold particles again reveal an abundance of ISG within the flagellar hillocks. Labels as in Figs 1, 3. Bars, 100 nm.
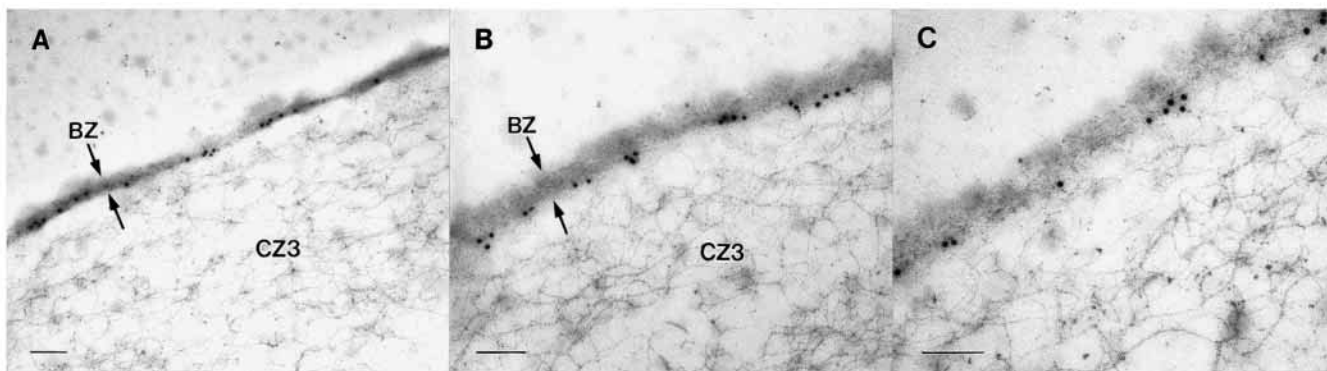
Fig. 6. Immunolocalization of ISG in the boundary zone (BZ) of 18-hour-old spheroids, in three independent experiments. All sections are cut perpendicular to the surface of the spheroids. Numerous gold particles reveal the presence of ISG at the inner edge of the boundary zone (BZ3). Bars, 100 nm.

Therefore, it was impossible to determine whether such a 'dominant-negative' form of ISG might be able to disrupt spheroid organization at any time in the life cycle, or whether it might only have such an effect if present at some critical developmental period. To address such questions, we initiated

studies with a different agent of this type, namely CTD: the synthetic form of the C-terminal decapeptide of ISG, KKKATGRRLL. It was previously shown that *V. carteri* cultures exposed to the CTD for 24-48 hours exhibited serious morphological defects, presumably as a consequence of the

Fig. 7. The truncated ISG: physical map of the truncated gene, stage-specific synthesis of the corresponding mRNA in transformants, and nucleotide sequence of a 224-bp cDNA-fragment coming from the truncated ISG mRNA. (A) Structure of the truncated ISG gene. Diagram indicating the proposed deletion; tsp: transcription start point; E1-3: exons 1-3. The beginning and end of the region to be deleted are marked in the diagram of the wild-type gene with vertical arrowheads and in the truncated gene by (Δ). The plan was to remove exon 2 (E2), which encodes most of the N-terminal, globular domain of ISG (residues 13 to 212 of the mature ISG; see Ertl et al., 1992). Small horizontal arrows below the diagram of the truncated gene show the positions of oligonucleotide primers used for RT-PCR of putative transformants. (B) Stage-specific synthesis of truncated ISG mRNA in transformants. The truncated ISG mRNA was detected by reverse transcription and subsequent PCR amplification (RT-PCR). A 224-bp cDNA fragment of the truncated ISG mRNA was expected if the intron within this fragment was spliced correctly. The truncated ISG mRNA was only detectable in four of the nine transformants that had been transformed with the truncated ISG gene. The result with one of these four transformants is shown (Transformant) and compared to the parent untransformed strain 153-48 (Parent strain 153-48). (C) Nucleotide sequence (with deduced amino acid sequence below it) of the 224-bp cDNA obtained by RT-PCR of RNA at the stage of inversion from the four independent isolates mentioned above that had been transformed with the putative truncated ISG gene, using primers corresponding to the regions indicated by horizontal arrows. The sequence obtained indicates that the deletion (at the position marked Δ) was successful, and that the remaining intron (previously located at the position marked by a vertical arrow) was removed correctly by the splicing machinery of *Volvox*. The vertical arrowhead denotes the signal peptidase cleavage site.
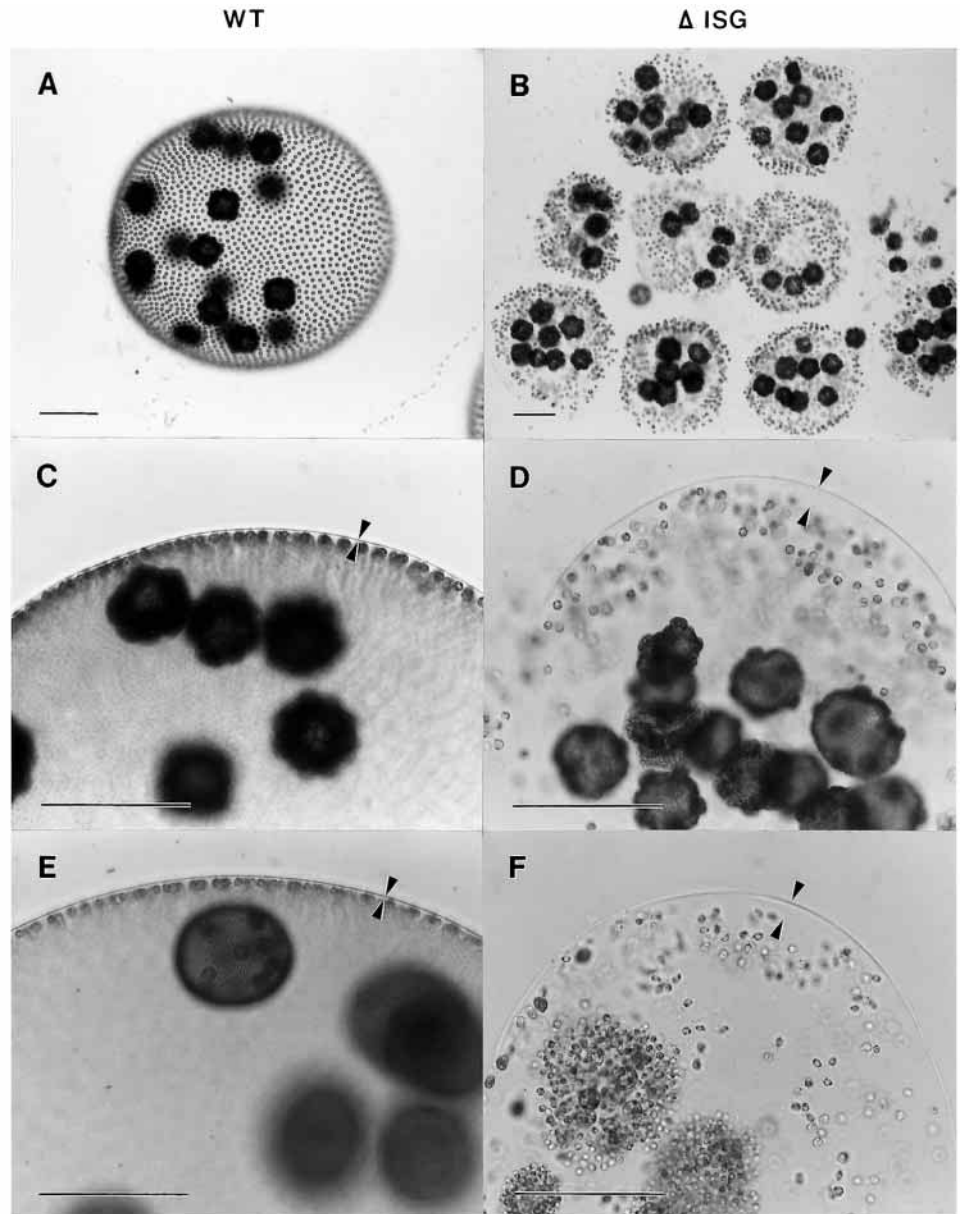
WT　　　　Δ ISG
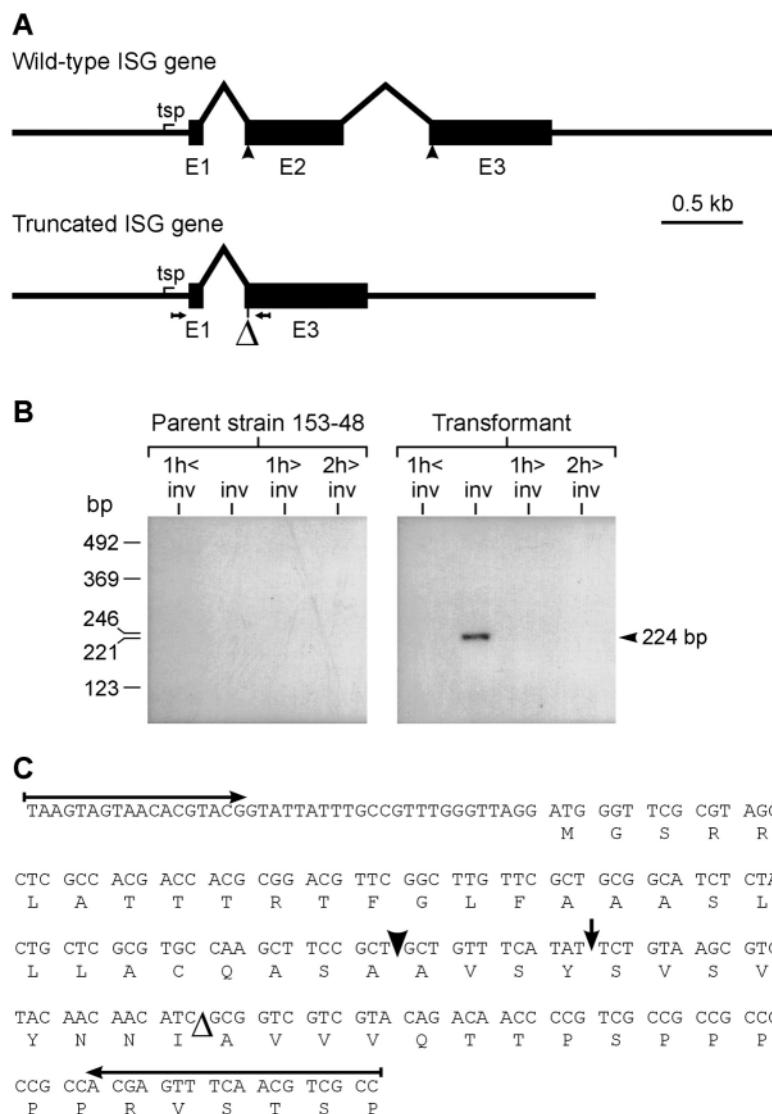
Fig. 8. Light micrographs contrasting certain morphological features of wild-type *V. carteri* spheroids (WT: A,C,E) with those of transformants expressing the truncated ISG gene (ΔISG: B,D,F). In A-D, cleaving, preinversion embryos are present inside each of the parental spheroids, whereas in E and F postinversion juveniles are present inside each parent. As long as the transgenic embryos are in the preinversion stage – and thus held together by cytoplasmic bridges – they look normal (B,D). But after inversion – when cytoplasmic bridges have broken down and the task of holding the cells in a regular arrangement should have been assumed by the ECM – the transgenic progeny look totally disorganized (F), and this disorganized condition persists into the adult stages. Arrowheads in C-F indicate that whereas the somatic cells are all normally located very close to the outer surface of the ECM (through which their flagella project) there is no regular spatial relationship between the somatic cells and the surface of the spheroid in the transgenic adults. Indeed, observation at higher power revealed that virtually all of the flagella of the transformants are trapped within the ECM, which explains why these organisms cannot swim. Labels as in Figs 1, 3. Bars, 100 mm.

effect of the peptide on ECM assembly (Ertl et al., 1992). But more detailed studies of the time course and mechanism of action of CTD were not reported.

　We exposed inverting *Volvox* embryos to medium containing 0.5 mM CTD, washed out the peptide at 0.5 or 5 hours, and then examined the resulting spheroids when they were at the 15-hours-postinversion stage. Spheroids that had been exposed to CTD for only 30 minutes had a somewhat variable phenotype, but even individuals that superficially resembled untreated spheroids were unable to swim. When such individuals were examined with differential interference contrast optics, it became obvious why this was the case: their flagella (although normal in length and motility) were buried deeply within a mass of abnormal matrix material that extended outward, far beyond the edges of the somatic cells (Fig. 10B). Incubation with CTD for 5 hours caused much greater abnormalities of ECM (and hence spheroid) architecture: As in *V. carteri* individuals expressing the truncated version of the ISG gene, *V. carteri* that had been

exposed to CTD for 5 hours in the postinversion period appear to lack nearly all elements of normal spheroid organization (Fig. 10C,D); at higher magnification it is clear that the orientation of individual somatic cells in such spheroids is entirely random (not shown). Moreover, the spheroids remain very small, indicating that the ECM doesn't expand normally. In addition, the outer surface of such individuals is extremely sticky, so that they tend to adhere tightly to one another or to certain plastic surfaces (which wild-type spheroids never do). Despite all these defects of spheroid organization, both the somatic cells and the gonidia (considered individually) are normal in size, and apparently quite healthy.

　We have used several commercially available basic peptides, such as GK, LRRASLG, and KKGE as controls. These peptides did not affect ECM assembly at all.

　The nature of the ECM perturbations induced by CTD exposure were assessed by fine structure immunocytochemistry of 15-hours-postinversion spheroids that had been exposed to CTD as in the preceding experiment.
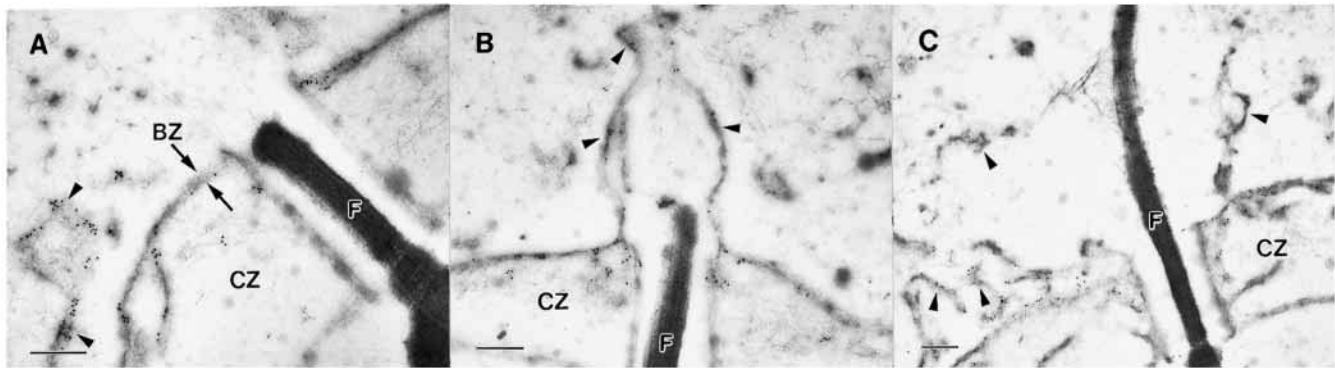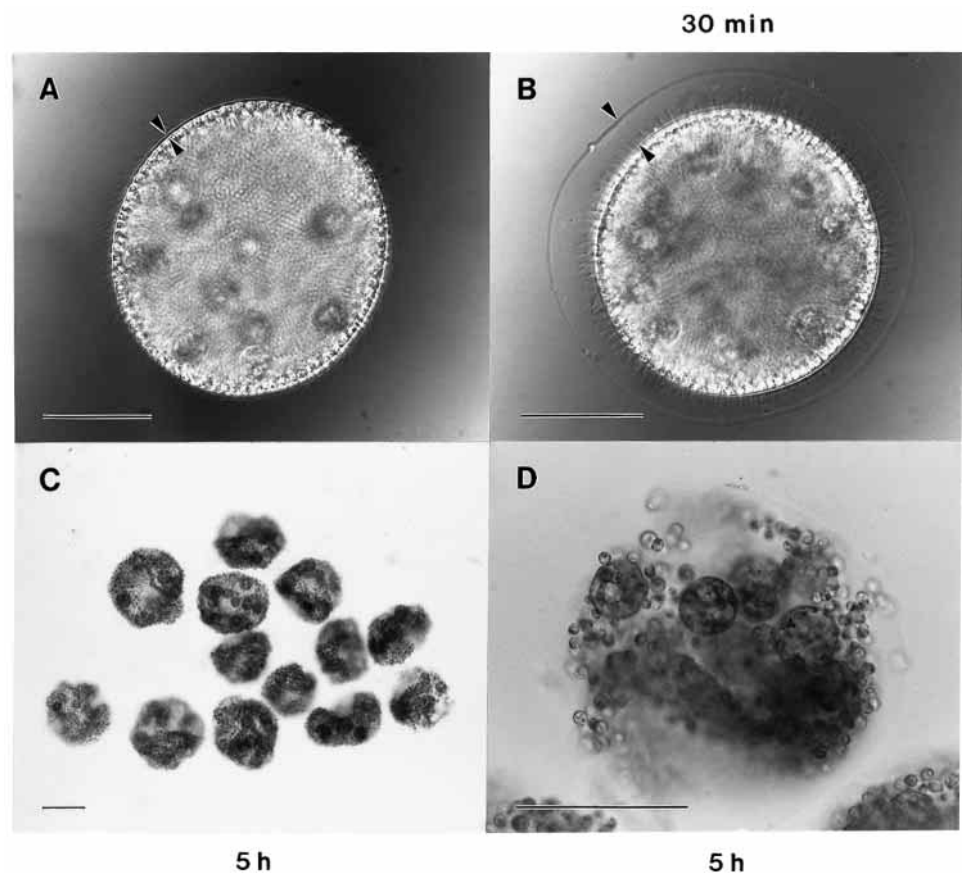
Fig. 9. Immunolocalization of ISG in 18-hour-old transgenic juveniles expressing the truncated ISG gene. As in Fig. 4, all three sections pass longitudinally through a flagellum. Note that there are no flagellar hillocks resembling those of wild-type juveniles of comparable age (Fig. 4). Although there are short regions where the boundary zone appears relatively normal (arrows labeled BZ in A), additional boundary zone-like elements that contain gold grains indicating the presence of ISG are also present in chaotic, wholly unpredictable arrays (arrowheads), many of which extend outward into the environment well beyond the position where the outer surface of the ECM would normally be located. Furthermore, the cellular zone (CZ) of the transgenic ECM seems to contain much less fibrous material than in wild-type *Volvox* of comparable age. Labels as in Figs 1, 3. Bars, 300 nm.

In addition, spheroids that had been exposed to CTD for the entire 15-hour period were also examined. The results indicated that even spheroids that had been exposed to the agent for as little as 30-minutes were unable to construct normal flagellar hillocks, or construct a boundary zone that truly acted as a boundary zone and prevented deposition of ECM components at greater distance from the somatic cells (Fig. 11A). Indeed, the ECM of such spheroids appears so thoroughly disorganized at this level of analysis it becomes difficult to say whether the ECM defects are any worse in spheroids that were exposed to CTD for 5 hours (Fig. 11B) or 15 hours (Fig. 11C). Nevertheless, low power views such as those shown in Fig. 10 reveal that there really is a substantial difference. Despite the kind of organization defects in the ECM that are seen at the EM level in organisms exposed to CTD for only 30 minutes (Fig. 11A), somehow the somatic cells of these spheroids often continue to be held in relatively normal orientations relative to one another (Fig. 10A). In contrast, in spheroids that were exposed to the peptide for 5 hours, there is nothing normal about the orientations of the somatic cells.

Fig. 10. Light micrographs contrasting morphological features of a control *V. carteri* spheroid (A) with those of individuals that had been exposed to CTD, the synthetic C-terminal decapeptide of ISG (B-D). CTD (0.5 mM) was added to wild-type embryos at the time of inversion for 30 minutes or 5 hours; then the peptide was washed away and the algae were incubated in standard medium until they reached the 15 hours-postinversion stage. Whereas the edge of the ECM is very close to the somatic cells in control spheroids (arrowheads in A), it is far away from the somatic cells in individuals that were exposed to the decapeptide for only 30 minutes at the time of inversion (arrowheads in B). With their flagella trapped within the ECM like this, it is not surprising that such spheroids cannot swim. Incubation with CTD for a longer period (5 hours) leads to a severely disorganized ECM and spheroids in which the cells are oriented in an apparently random manner (C,D). These algae are also unable to swim. (A,B) Nomarski differential interference contrast optics; (C,D) bright-field optics. Bars, 100 μm.
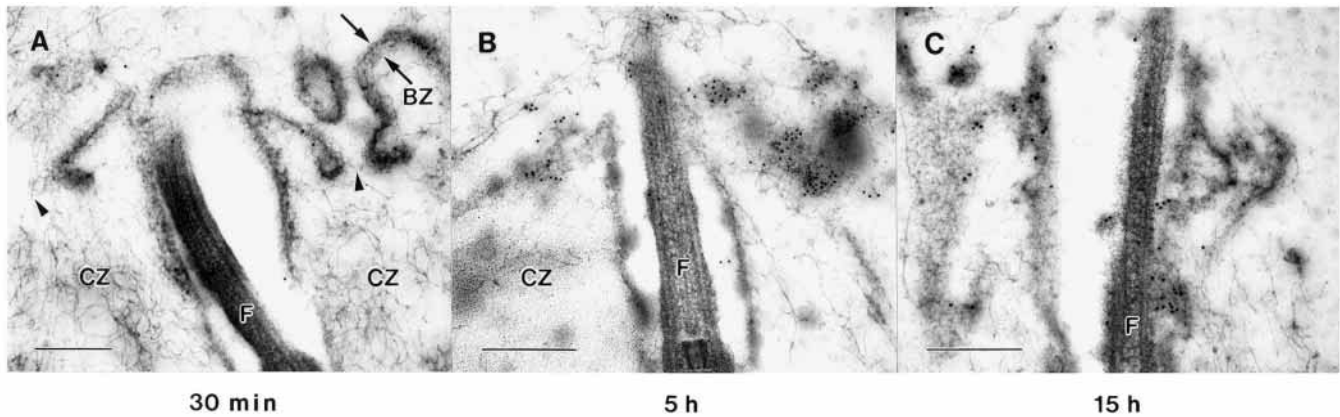
30 min   5 h   15 h

Fig. 11. Immunolocalization of ISG in cross sections of wild-type juveniles that were exposed to 0.5 mM CTD at the time of inversion. The peptide was washed away after 30 minutes (A), after 5 hours (B), or not at all (C), and the algae were all incubated until they had reached the 15 hours-postinversion stage. All sections pass longitudinally through a flagellum. The spheroids have no flagellar hillocks and the entire ECM looks disorganized; it does not stop at the area where the boundary zone is normally located, but extends much further outward. Immunogold labeling indicates that the ISG-containing part of the boundary zone is intermixed with other ECM components and no longer builds a distinct spheroid border. Arrowheads in A indicate that even after incubation with the CTD for only 30 minutes there is no longer a continuous BZ. Labels as in Figs 1, 3. Bars, 300 nm.

Indeed, in spheroids incubated with the peptide for 5 hours there are often neighboring somatic cells that are oriented in directions differing by as much as 180°.

These observations raise the question of whether there is a critical period for CTD action, and if so, when it might be. The fact that the ECM abnormalities caused by even a 30-minute exposure to CTD during inversion resulted in spheroids unable to swim suggested that motility might be used as an endpoint in an experiment designed to address this question. Therefore, we exposed aliquots of sibling embryos/juveniles to 0.5 mM CTD for 30 minute periods beginning before, during, and at various intervals after inversion, and then assessed the ability of the resulting spheroids to swim when they had reached the 24-hours-postinversion stage. The results (Table 1) clearly indicated that by this criterion the embryos are insensitive to CTD before inversion begins, are maximally sensitive to it at the time that ISG synthesis begins (during inversion and immediately thereafter), have become largely insensitive to it by 2 hours postinversion, and completely insensitive to it by 4 hours postinversion. We conclude that the ISG-derived decapeptide probably is able to perturb only the early steps of ECM assembly.

It is impossible to completely rule out the possibility that other ECM molecules might contain the KKKATGRRLL decapeptide sequence. But because (i) an anti-decapeptide antibody detects only the single band corresponding to ISG on a western blot, (ii) the sequence is not found in any other protein in the SWISS PROT database and (iii) *Volvox* is only sensitive to the decapeptide during and immediately after the time when ISG is being synthesized and assembled, it seems extremely unlikely that the effects of the decapeptide are mediated by some other molecule.

DISCUSSION

The first indications that ISG might play some particularly important role in *V. carteri* ECM biogenesis came with the discovery that it appeared to be the first ECM glycoprotein to

be synthesized in the asexual life cycle (Schlipfenbacher et al., 1986; Wenzl and Sumper, 1982). This presumption about the possible importance of ISG was reinforced when it was subsequently reported that the message encoding ISG was synthesized only during an ~10 minute period during embryo inversion, and that prolonged cultivation of the organism in the presence of a peptide corresponding to the C-terminal decapeptide of ISG (here called CTD) caused major perturbations of ECM organization and spheroid morphogenesis (Ertl et al., 1992) (although that study indicated that ISG mRNA is synthesized for only for 10 minutes during inversion, the present study indicates that ISG continues to accumulate in the ECM for several hours beyond that). However, intriguing as the latter report was, it provided little insight into exactly what role ISG might play in *V. carteri* development.

Here we provide experimental evidence indicating that ISG acts as a key organizer of ECM architecture in *V. carteri*, and that this organizer function of ISG is essential for assuring that somatic cells of postinversion *V. carteri* spheroids are held in orientations and locations that makes adaptive swimming behavior possible.

The fine-structure immunolocalization studies that are reported here indicate that immediately after inversion – and before any other features of the ECM can be detected in the electron microscope – ISG is already present in significant abundance at the bases of the flagella of somatic cells, in the

Table 1. Stage-dependent sensitivity of isolated *Volvox* juveniles to CTD

Stage of development at beginning of 30-minute exposure to CTD	Percentage of spheroids able to swim a day later
Negative control; no CTD	98%
1 hour prior to inversion	89%
During inversion	0%
1 hour after inversion	12%
2 hours after inversion	64%
3 hours after inversion	82%
4 hours after inversion	99%
15 hours after inversion	97%

position where the flagella hillock, FZ3a, will subsequently be located (Fig. 3A). Shortly thereafter, ISG is also present in the developing boundary zone, particularly in two regions: (i) where the BZ abuts the flagellar hillock, FZ3a (Fig. 3C), and (ii) at the 3-way junction where the BZ meets the nascent portion of CZ3 that will become the common side wall joining two adjacent cellular compartments (Fig. 3D). As the BZ becomes thicker, and as more ISG accumulates in it, it becomes clearer that ISG is not located throughout the BZ, but is specifically localized on its inner face: BZ3 (Fig. 6). Thus, one of the first ECM elements to be formed in the postinversion period is what we may call 'the ISG-based FZ3a–BZ3 complex.'

As mentioned in the introduction, immunofluorescence images included in an earlier report (Ertl et al., 1992) revealed that ISG is located in the ECM, near the surface of the spheroid (presumably somewhere in or near the boundary zone) and in the vicinity of the flagellar bases. It was the low resolution of such immunofluorescence studies that provided one of the primary motivations for performing the EM immunolocalization studies reported here. However, the immunofluorescence data are fully consistent with the EM immunolocalization data shown in Figs 4, 5.

What may be the significance of the fact that the first ECM structure that can be detected in the postinversion embryo is the flagellar hillock (FZ3a), and that this quickly becomes incorporated into what we have just called 'the ISG-based FZ3a–BZ3 complex'? An insight that we believe is highly relevant comes from a study performed some years ago by Robert Huskey with a temperature-sensitive-flagellaless mutant (Huskey, 1979). Huskey showed that if this mutant was cultured at the permissive temperature at the end of inversion – so that flagella would be present at the time that ECM assembly was beginning and the cytoplasmic bridges were breaking down – then the ECM formed in such a way that all of the somatic cells were aligned similarly along the anterior-posterior axis of the spheroid (just as they had been in the developing embryo), and thus the spheroid exhibited normal swimming behavior. In contrast, if the mutant was incubated at restrictive temperature at the end of inversion – so that flagella were *not* present at the time that ECM assembly began – the normal alignment of the somatic cells was lost, and they came to be oriented randomly within the spheroid. As a result, although these somatic cells produced normal flagella when they were shifted to the permissive temperature, these flagella could not be used to provide normal swimming behavior, because they were oriented (and hence beating) in all sorts of random directions. The conclusions to be drawn from Huskey's study are (i) that adaptive swimming behavior in *V. carteri* depends upon all of the somatic cells being properly aligned within the ECM (as they are initially within the embryo), and (ii) that the somatic cells can be held in such orientations when the cytoplasmic bridges break down only if flagella have been present during the initial stages of ECM deposition.

At the time that the Huskey study was published, it was not at all clear how the flagella might play this key role of stabilizing somatic cell alignments during the early stages of ECM assembly. But the observations made here appear to provide an explanation. Our working hypothesis now is that the ISG-based FZ3a–BZ3 complex that is formed immediately after inversion constitutes the initial framework that serves to lock somatic cells in place via their flagella, while simultaneously serving as the scaffold upon which the rest of the ECM is organized.

The effects that we observed when ISG function was interfered with by either of two methods (by expression of the truncated ISG transgene, or by incubation in the presence of the C-terminal decapeptide of ISG) are fully consistent with the foregoing hypothesis. In both cases, three principal effects were observed that are of just the sort that the above hypothesis predicts should occur when ISG function is inhibited: (i) neither the flagellar hillocks nor the boundary zone formed normally; (ii) the somatic cells were not held in proper orientation, and (iii) the rest of the ECM – most of which never contains ISG – was as disorganized as the regions that normally do contain abundant ISG (Figs 8-11). It is also noteworthy that following both of these treatments ECM components (albeit highly disorganized ones) are found well out beyond the position where the boundary zone is normally located. This indicates to us that one of the functions of the BZ is to act as a barrier that restricts the outward diffusion of ECM components.

How do the truncated ISG molecules that are encoded by the transgene, and the C-terminal decapeptide (CTD) exert their drastic effects on ECM assembly? A likely possibility is that both of them act as dominant-negative inhibitors of an ISG cross-linking activity because they both possess a protein-binding site that is located at the C-terminal end of the ISG molecule, but lack the binding site that has been inferred to exist in the amino-terminal domain (Ertl et al., 1992). In any case, because the CTD can so easily be added to and withdrawn from cultures, it has provided us with the opportunity to determine when and for how long ECM assembly can be perturbed by addition of an ISG inhibitor. The answer seems clear (Table 1): the embryo first becomes sensitive to CTD inhibition during inversion (at the time when ISG is first being synthesized) and then rapidly loses sensitivity to the agent ~3 hours later (as soon as the 'ISG-based FZ3a–BZ3 complex' has become well formed; Fig. 3). This result supports our hypothesis that the only essential function ISG executes in *V. carteri* morphogenesis is in formation of the FZ3a–BZ3 complex as the first step in ECM assembly. Nevertheless, this truly is an essential function, because, as our inhibitor studies show, in the absence of the ISG-based FZ3a–BZ3 complex a disorganized spheroid is produced that cannot swim, and therefore could not survive in the wild.

REFERENCES

Adair, W. S., Steinmetz, S. A., Mattson, D. M., Goodenough, U. W. and Heuser, J. E. (1987). Nucleated assembly of *Chlamydomonas* and *Volvox* cell walls. *J. Cell Biol.* **105**, 2373-2382.

Ertl, H., Hallmann, A., Wenzl, S. and Sumper, M. (1992). A novel extensin that may organize extracellular matrix biogenesis in *Volvox carteri*. *EMBO J.* **11**, 2055-2062.

Hallmann, A. and Sumper, M. (1994). Reporter genes and highly regulated promoters as tools for transformation experiments in *Volvox carteri*. *Proc. Nat. Acad. Sci. USA* **91**, 11562-11566.

Hallmann, A., Rappel, A. and Sumper, M. (1997). Gene replacement by homologous recombination in the multicellular green alga *Volvox carteri*. *Proc. Nat. Acad. Sci. USA* **94**, 7469-7474.

Hallmann, A., Godl, K., Wenzl, S. and Sumper, M. (1998). The highly efficient sex-inducing pheromone system of *Volvox*. *Trends Microbiol.* **6**, 185-189.

Horton, R. M., Hunt, H. D., Ho, S. N., Pullen, J. K. and Pease, L. R. (1989). Engineering hybrid genes without the use of restriction enzymes: gene splicing by overlap extension. *Gene* **77**, 61-68.

Huskey, R. J. (1979). Mutants affecting vegetative cell orientation in *Volvox carteri*. *Dev. Biol.* **72**, 236-243.

Kirk, D. L. and Kirk, M. M. (1983). Protein synthetic patterns during the asexual life cycle of *Volvox carteri*. *Dev. Biol.* **96**, 493-506.

Kirk, D. L., Birchem, R. and King, N. (1986). The extracellular matrix of *Volvox*: a comparative study and proposed system of nomenclature. *J. Cell Sci.* **80**, 207-231.

Kirk, D. L. (1998). *Volvox*: Molecular-genetic origins of multicellularity and cellular differentiation, developmental and cell biology series. Cambridge: Cambridge University Press.

Kirk, D. L. (1999). Evolution of multicellularity in the volvocine algae. *Curr. Opin. Plant Biol.* **2**, 496-501.

Kirk, M. M. and Kirk, D. L. (1985). Translational regulation of protein synthesis, in response to light, at a critical stage of *Volvox* development. *Cell* **41**, 419-428.

Koufopanou, V. and Bell, G. (1993). Soma and germ: An experimental approach using *Volvox. Proc. R. Soc. Lond. Ser. B. Biol. Sci.* **254**, 107-113.

Luft, J. H. (1964). Electron microscopy of cell extraneous coats as revealed by ruthenium red staining. *J. Cell Biol.* **23**, 54A.

Provasoli, L. and Pintner, I. J. (1959). Artificial media for freshwater algae: problems and suggestions. In *The Ecology of Algae* (ed. C. A. Tyron and R. T. Hartman), pp. 84-96. Pittsburgh, PA: Pymatuning Laboratory of Field Biology, Special Publication no. 2, University of Pittsburgh.

Rausch, H., Larsen, N. and Schmitt, R. (1989). Phylogenetic relationships of the green alga *Volvox carteri* deduced from small-subunit ribosomal RNA comparisons. *J. Mol. Evol.* **29**, 255-265.

Sambrook, J., Fritsch, E. F. and Maniatis, T. (1989). *Molecular Cloning: A Laboratory Manual.* Cold Spring Harbor, NY: Cold Spring Harbor Laboratory Press.

Schiedlmeier, B., Schmitt, R., Müller, W., Kirk, M. M., Gruber, H., Mages, W. and Kirk, D. L. (1994). Nuclear transformation of *Volvox carteri*. *Proc. Nat. Acad. Sci. USA* **91**, 5080-5084.

Schlipfenbacher, R., Wenzl, S., Lottspeich, F. and Sumper, M. (1986). An extremely hydroxyproline-rich glycoprotein is expressed in inverting *Volvox* embryos. *FEBS Lett.* **209**, 57-62.

Starr, R. C. (1969). Structure, reproduction, and differentiation in *Volvox carteri* f. *nagariensis* Iyengar, strains HK9 & 10. *Arch. Protistenk.* **111**, 204-222.

Starr, R. C. (1970). Control of differentiation in *Volvox. Dev. Biol. Suppl.* **4**, 59-100.

Starr, R. C. and Jaenicke, L. (1974). Purification and characterization of the hormone initiating sexual morphogenesis in *Volvox carteri* f. *nagariensis* Iyengar. *Proc. Nat. Acad. Sci. USA* **71**, 1050-1054.

Starr, R. C. (1980). Colonial chlorophytes. In *Phytoflagellates* (ed. E. R. Cox), pp. 147-63. Amsterdam: Elsevier.

Sumper, M. and Hallmann, A. (1998). Biochemistry of the extracellular matrix of *Volvox. Int. Rev. Cytol.* **180**, 51-85.

Venable, J. H. and Coggeshall, R. (1965). A simplified lead citrate stain for use in electron microscopy. *J. Cell Biol.* **25**, 407-408.

Viamontes, G. I., Fochtmann, L. J. and Kirk, D. L. (1979). Morphogenesis in *Volvox*: analysis of critical variables. *Cell* **17**, 537-550.

Wenzl, S. and Sumper, M. (1982). The occurrence of different sulphated cell surface glycoproteins correlates with defined developmental events in *Volvox. FEBS Lett.* **143**, 311-315.

Wenzl, S. and Sumper, M. (1987). Pheromone-inducible glycoproteins of the extracellular matrix of *Volvox* and their possible role in sexual induction. In *Algal Development (Molecular and Cellular Aspects)*, (ed. W. Wiessner, D. G. Robinson and R. C. Starr), pp. 58-65. Berlin: Springer-Verlag.

Woessner, J. P., Molendijk, A. J., van Egmond, P., Klis, F. M., Goodenough, U. W. and Haring, M. A. (1994). Domain conservation in several volvocalean cell wall proteins. *Plant Mol. Biol.* **26**, 947-960.